CTH-IEF-1988-16 ISSN

ANALYTICAL MODELS FOR PREDICTING THE ION VELOCITY DISTRIBUTIONS IN JET IN THE PRESENCE OF ICRF HEATING

BY

D. ANDERSON, L.-G. ERIKSSON, AND M. LISAK

INSTITUTIONEN FÖR ELEKTROMAGNETISK FÄLTTEORI

CHALMERS TEKNISKA HÖGSKOLA

ANALYTICAL MODELS FOR PREDICTING THE ION VELOCITY DISTRIBUTIONS IN JET IN THE PRESENCE OF ICRF HEATING

D. Anderson, L.-G. Eriksson, and M. Lisak

Institute for Electromagnetic Field Theory
and EURATOM Fusion Research (SERC)
Chalmers University of Technology
S-412 96 Göteborg, Sweden

The present report summarizes the work performed within the contract JT4/9008, the aim of which is to derive analytical models for ion velocity distributions resulting from ICRF heating on JET. The work has been performed over a two-year-period ending in August 1986 and has involved a total effort of 2.4 man years.

Introduction

Ion cyclotron heating has become a reliable method for supplementary heating in large plasma experiments. Its flexibility and great technological potential makes it one of the major alternatives for heating in future fusion reactors. In most experiments the fast magnetoacoustic wave is launched by the antenna and the damping of the wave occurs either directly by ion cyclotron and electron Landau damping or via a mode conversion process. In the present context we focus our attention on the case of direct absorption by ion cyclotron damping and in particular the concomitant distortion of the velocity distribution of the heated ions. The most prominent feature of this distortion is the high energy tails that are created, preferentially in the velocity coordinate perpendicular to the magnetic field.

Deviations from thermal Maxwellian form play an important role in determining many "secondary" physical quantities and processes, e.g. fusion reactivity, RF power absorption efficiency, high energy particle losses, RF-driven wave-particle instabilities, as well as for the interpretation of data from charge-exchange and neutron measurements.

Most of the analytical understanding of the effects of ICRH on the velocity distribution of the heated ions is provided by the classical paper by Stix, [1], from 1975. However, this paper is restricted to the minority heating scheme using the fundamental ion cyclotron resonance frequency and the subsequent development in the field of ICRH has emphasized several new aspects and heating scenarii, in particular majority heating at the second harmonic ion cyclotron resonance frequency, combined neutral beam and RF-heating scenarii, trapped particle effects and the time dependent behaviour of the velocity distributions. Extensive computer studies have also been made of the Fokker-Planck equation describing the RF-driven, quasi-linear diffusion processes which deform the velocity distribution. However, this effort has been dominated by numerical calculations and/or codes that are too cumbersome for routine use in situations where the distribution function itself is not of primary interest, but only the means to determine other plasma properties, e.g. plasma transport.

Thus, there is a great need for analytical or semi-analytical models that provide short computational procedure and contribute to the physical understanding of the effect of ICRH on the velocity distribution of the heated ions. The general objective of the work within the present contract is to contribute to this goal.

The more specific goals of the present work is to obtain theoretical models for ion distributions in various RF-heating schemes for JET as well as for the collisional power transfer to the background plasma particles. Particular emphasis has been given to the following points:

(i) the properties of the high energy anisotropic ion tails

(ii) majority heating at the second harmonic ion cyclotron resonance frequency

(iii) the pitch angle dependence of the RF-heated distribution functions

(iv) energy clamping scenarii involving ICRH and NBI with the RF wave tuned to the first or second harmonic cyclotron frequency of the injected ions

(v) the relevance of stationary solutions and extensions to non-stationary situations when necessary

(vi) formulation and analysis of a bounce-averaged Fokker-Planck equation which includes toroidal effects on ICRH.

A general description of the content of the work performed within the contract and results obtained in the different problem areas can be given as follows:

A. Properties of high energy anisotropic ion tails

In an introductory investigation, [2-4], we extended the steady-state analysis of Stix, [1], to include heating at the second harmonic ion cyclotron frequency and in particular finite Larmor radius effects which later

proved to play an important role for the ICRF heating scenarii on JET. Special emphasis in this investigation was given to the properties of the high energy strongly anisotropic tails and important information about the anisotropy in terms of perpendicular and parallel temperatures were obtained.

B. Analysis and use of pitch angle averaged distributions

In a subsequent investigation [5-9] we assumed the distribution function to be essentially isotropic and derived analytical and computationally simple semi-analytical approximations for the ion distributions resulting from ICRH as well as from energy clamping involving ICRH and NBI. The result was used to evaluate the weighted velocity space averages of the distribution, which determine the fusion reactivity and the collisional power transfer to plasma background particles and to study their scaling with RF-parameters like absorbed power and perpendicular wave number. The importance of higher order finite Larmor radius effects for the formation of RF-induced high energy tails was particularly emphasized. Comparison based on full 2D numerical calculations showed very good agreement with the semi-analytical results.

In a further analysis [10-11], using a completely new approach, we derived an equation for the pitch angle averaged distribution which actually is all that is needed for the evaluation of velocity space averages involving pitch angle independent weighting functions. The subsequent solution reconciled, in a consistent manner, previous complementary results based on assumptions of either isotropic or strongly anisotropic distributions.

C. Effects of particle trapping on ICRH

A new bounce averaged Fokker-Planck equation, accounting for the effect of particle trapping, was derived in [12]. This equation was subsequently analyzed in [13] using a perturbative expansion in generalized Legendre polynomials. It was found that trapped particle effects tended to reduce the overall anisotropy of the distribution, but that they should have little effect on the isotropic bulk distribution. This in turn implies little effect on most velocity space averages.

D. Collisionless short time evolution of ion distributions in the presence of ICRH

Problems in connection with RF-enhanced sawtooth activity, which involve very short time scales, have focussed the interest on the short time development of RF-heated ion distributions. In [11,14,15] we derived explicit analytical solutions for the collisionless evolution of ion distributions for heating scenari involving conventional ICRH as well as for energy clamping schemes. The effect of particle trapping on the time evolution of the ion distributions was also analyzed.

A more detailed presentation of our results is given in the following paragraphs.

Qualitative picture of RF-driven velocity space diffusion

The most prominent features of distribution functions resulting from velocity space diffusion due to ICRH can be understood as follows:

In the simplest picture of the ICRH absorption mechanism, an ion following a magnetic field line receives a small change, $\Delta v_\perp$, of its perpendicular velocity each time it passes through the resonance layer. During the time, τ, between two consequtive velocity changes phase correlation is destroyed by collisions and/or collisionfree stochasticity and the particle performs a random walk in velocity space. The corresponding diffusion coefficient, D, can be estimated as

$$D \sim \frac{(\Delta v_\perp)^2}{\tau} = \frac{2\Delta E_\perp}{m\tau} = \frac{2P}{mn} \qquad (1)$$

where $\Delta E_\perp = \frac{1}{2} m(\Delta v_\perp)^2$ is the change in perpendicular energy of the particle, P is the absorbed RF power density, and n is the density of absorbing ions.

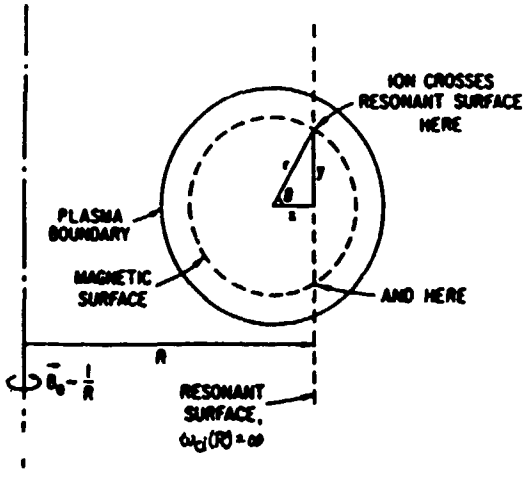

Fig. 1 Geometry for ion cyclotron resonance in a Tokamak, [1].

During the initial evolution of the distribution function, f, of the heated ions, collisional effects can be neglected and we obtain the following equation for the RF-induced velocity diffusion

$$\frac{\partial f}{\partial t} = \frac{1}{v_\perp}\frac{\partial}{\partial v_\perp}\left(Dv_\perp \frac{\partial f}{\partial v_\perp}\right) \tag{2}$$

In the case of ICRH using the fundamental ion cyclotron frequency, the diffusion constant is independent of $v_\perp$ (for not too high energies). The solution of eq. (2), subject to the initial condition of a Maxwellian distribution of the form $f(v_\perp, v_\parallel, 0) = A \exp(-v^2/v_m^2)$, is

$$f(v_\perp, v_\parallel, t) = \frac{A}{1+t/t_o} \exp\left[-\frac{v_\parallel^2}{v_m^2} - \frac{v_\perp^2}{v_m^2(1+t/t_o)}\right] \tag{3}$$

where we have introduced the characteristic tail formation time, t_o, as

$$t_o = \frac{v_m^2}{4D} = \frac{nT}{P_{RF}} \tag{4}$$

Here the temperature, T, is defined by $T = \frac{1}{2} mv_m^2$ and P_{RF} is the absorbed power density computed from eq. (2).

The solution (3) preserves the Maxwellian form but the unaffected parallel temperature in combination with the (linearly) increasing perpendicular temperature create an anisotropy in preference of the perpendicular velocity coordinate. It is particularly instructive to consider the evolution of the curves of constant f: the initial circles are transformed into ellipses with successively increasing elongation, cf. Fig. 2.

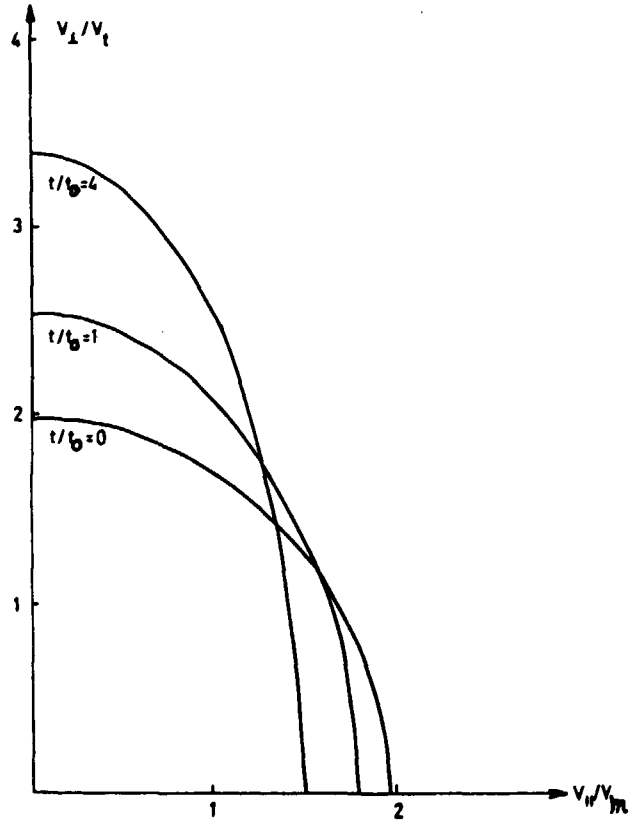

Fig. 2. Time development of curves of constant f.

Collisional effects will ultimately become important on time scales of the order of the slowing down time, t_s. A qualitative picture of the resulting stationary distribution function should be obtained by terminating the solution (3) at $t = t_s$. The important parameter determining the increase in the perpendicular temperature as well as the degree of anisotropy is then t_s/t_o, which apart from a numerical factor of order unity, corresponds

to the characteristic parameter, ξ, used by Stix, [1,2]. Actually

$$\xi = \frac{t_s}{3t_o} = \frac{t_s P_{RF}}{3nT} \tag{5}$$

However, a complication is introduced by the fact that the slowing down time will be very different for high and low energy ions, which slow down primarily on electrons and background ions respectively. The slowing down time for low energy ions is $(m_e/m_i)^{1/2}$ times smaller than t_s, where m_e and m_i denote the masses of electrons and background ions respectively. This has the important consequence that the temperature rise of the ICRF-heated low energy ions occur during a much shorter time and becomes correspondingly smaller.

For realistic absorbed RF powers we have the following inequality:

$$\frac{t_s}{t_o}\sqrt{\frac{m_e}{m_i}} \lesssim 1 \ll \frac{t_s}{t_o} \tag{6}$$

which implies that the bulk part of the distribution only experiences a small temperature rise whereas for high energies a strongly enhanced tail can be expected.

Similar arguments can be used to discuss the resulting anisotropy. In the low energy range, the small temperature rise and the strong pitch angle scattering should make the bulk distribution almost isotropic, although with a slight elongation in the perpendicular direction. In the high energy region, where the perpendicular temperature is strongly enhanced while pitch angle scattering becomes increasingly ineffective, a strong anisotropy can be expected.

Thus, we arrive at the following qualitative picture of the distribution function resulting from ICRH: the distribution should consist of an essentially isotropic bulk with an only slightly increased temperature, T_o, and an anisotropic high energy tail with strongly increased perpendicular temperature, $T_\perp \gg T_o$, but with only slightly increased parallel temperature,

$T_{\parallel} \gtrsim T_o$. The transition from bulk to tail can be expected to occur around the energy, E_c, at which electrons and ions contribute equally to the collisional friction force, i.e.

$$E_c \simeq 15\, T_b\, A\left(\Sigma \frac{n_j Z_j^2}{n_e A_j}\right)^{2/3} \tag{7}$$

where n_j, A_j, and Z_j denote the density, mass number and charge number respectively of the background ions, A is the mass number of the heated ions and n_e is the electron density.

The explicit solution of the RF-driven diffusion equation, as given by eq. (3), is only valid when D is a constant (heating at the fundamental ion cyclotron resonance frequency). In the case of second harmonic heating, the diffusion constant is proportional to the perpendicular energy of the particle. This should tend to make the bulk distribution even more isotropic and further enhance the anisotropy of the high energy tails.

The following figures illustrate the good agreement between the qualitative picture obtained here and various numerical and experimental results

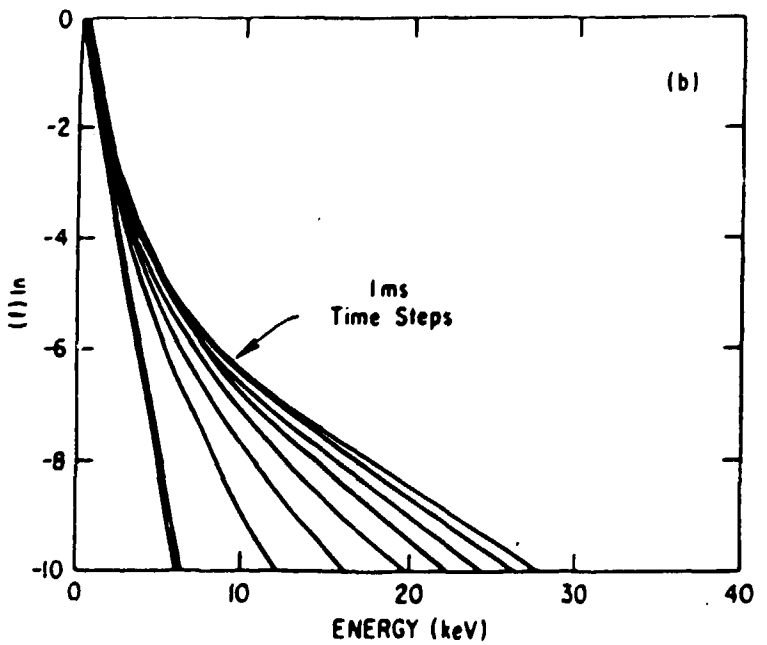

Fig. 3. Numerical solution of the time evolution of the distribution function, [16].

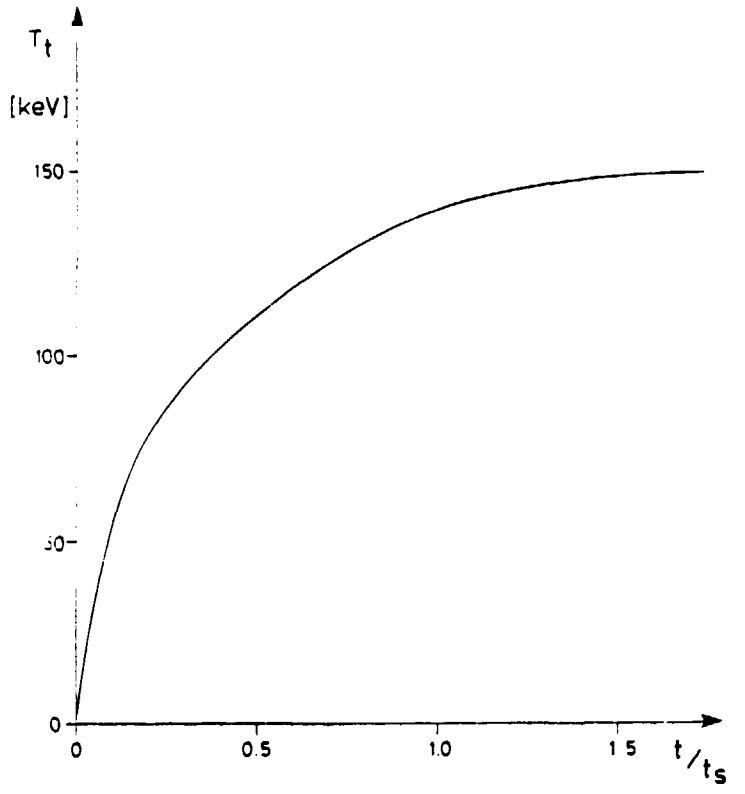

Fig. 4. Numerically obtained tail temperature evolution [7]. The initial linear rise is consistent with eq. (2).

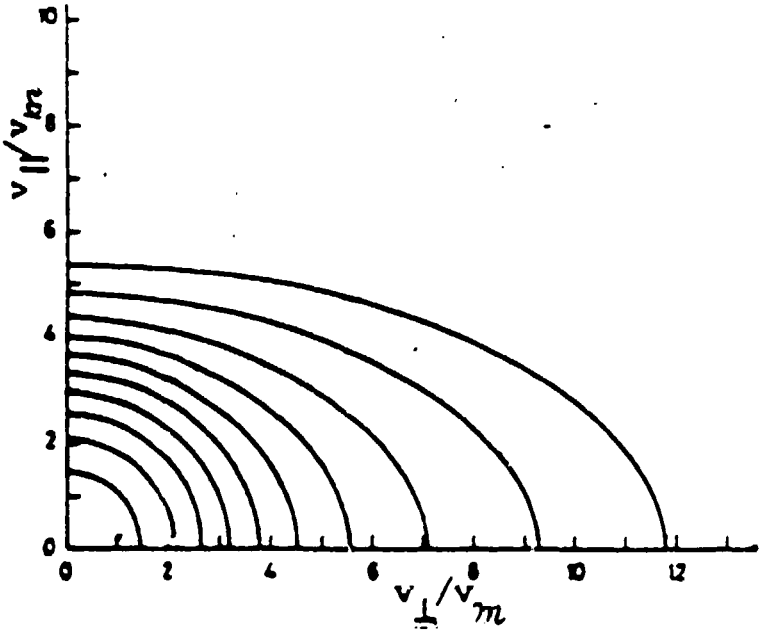

Fig. 5. Stationary level curves as obtained numerically in [17].

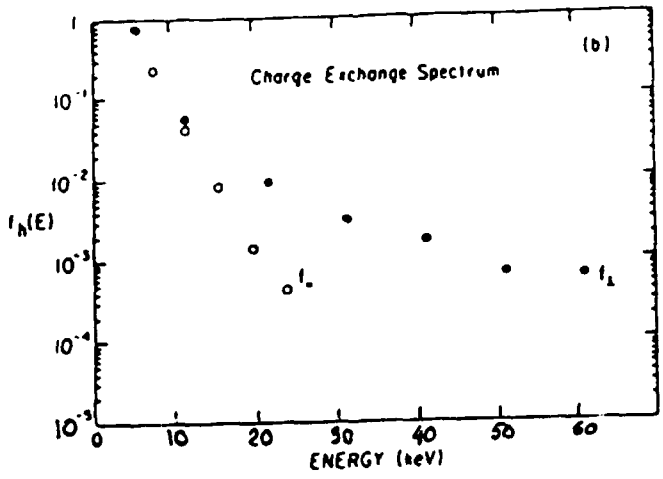

Fig. 6. Experimentally obtained charge exchange spectrum, [18].

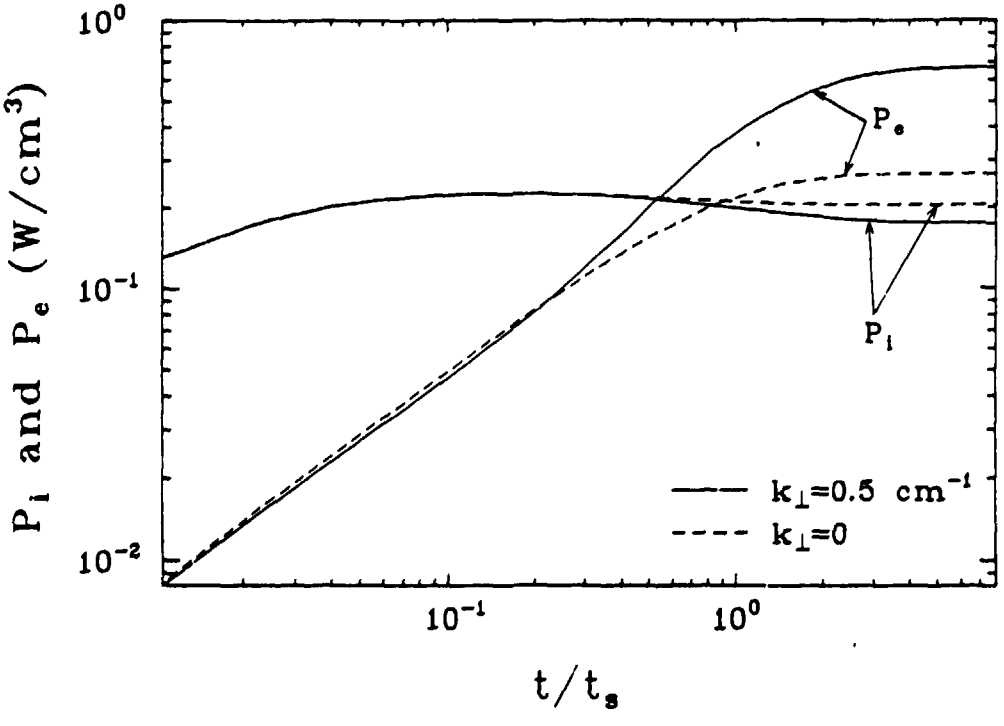

Fig. 7. Time evolution of absorbed RF power collisionally transferred to background ions, P_i, and electrons, P_e, [7].

Finally we emphasize that the different characteristic timescales to reach steady state for the bulk and tail respectively will reappear in derived quantities, e.g. the collisional power transfer to background ions should saturate much faster in time than the power transfer to the electrons, cf. Fig. 7.

Quantitative analysis - the Fokker-Planck quation

A quantitative analysis of the RF-induced distortion of the velocity distribution must be based on the Fokker-Planck equation:

$$\frac{\partial f}{\partial t} = C(f) + Q(f) \tag{7}$$

where C(f) and Q(f) denote the collision and RF diffusion operator respectively. C(f) is given by

$$C(f) = -\frac{1}{v^2}\left[\frac{\partial}{\partial v}\left(\alpha v^2 f\right)\right] + \frac{1}{2v^2}\frac{\partial}{\partial v}\left(\beta v^2 \frac{\partial f}{\partial v}\right)$$

$$+ \frac{\gamma}{4v^2}\frac{\partial}{\partial \mu}\left[(1-\mu^2)\frac{\partial f}{\partial \mu}\right] \tag{8}$$

$\mu = v_{\parallel}/v$ is the pitch angle coordinate and α, β, and γ are the coefficients of the collision operator, [1,2]. The RF-diffusion operator, Q(f), is given by

$$Q(f) = \frac{1}{v_\perp}\frac{\partial}{\partial v_\perp}\left(v_\perp D \frac{\partial f}{\partial v_\perp}\right) \tag{9}$$

where the diffusion coefficient, D, is

$$D = K_n H_n\left(\frac{k_\perp v_\perp}{\omega_{ci}}\right) \equiv K_n\left[|E_+|^2 J_{n-1}^2\left(\frac{k_\perp v_\perp}{\omega_{ci}}\right) + |E_-|^2 J_{n+1}^2\left(\frac{k_\perp v_\perp}{\omega_{ci}}\right)\right] \tag{10}$$

K_n is a numerical constant, $|E_+|$ and $|E_-|$ are the amplitudes of the left and right hand components of the RF-wave. $k_\perp$ is the perpendicular wave number of the RF wave, ω_{ci} is the ion cyclotron frequency, and J_{n-1} and J_{n+1} are the Bessel functions of order n-1 and n+1 respectively, where n denotes the heating mode (n=1 for fundamental and n=2 for second harmonic heating).

We emphasize that the operators C(f) and Q(f) in eqs. (8) and (9) are expressed in different variables, (v,μ) and $(v_\perp, v_\parallel)$ respectively. If we express C(f) in the variables $(v_\perp, v_\parallel)$ or Q(f) in the variables (v,μ), very complicated expressions are obtained. This "incompatibility" of the operators C(f) and Q(f) has been one of the major difficulties in analytical investigations of the Fokker-Planck equation, eq. (7).

The situation is further complicated by the fact that the distribution function obtained as a solution of eq. (7) consists of an almost isotropic Maxwellian low energy bulk part plus a strongly anisotropic high energy tail. Thus, although the variables (v,μ), being the natural variables for the collision operator, should be very useful in describing the bulk distribution, they are not very appropriate when analyzing the high energy tail. Conversely, the variables $(v_\perp, v_\parallel)$ being the natural variables of the RF-diffusion operator, are ideally suited for an analysis of the tail, but they become very awkward when used to analyze the bulk distribution.

The bulk part of the distribution, which tends to be almost isotropic, contains most of the heated particles. From this point of view it is natural to express f, C(f), and Q(f) in the variables (v,μ) and to expand $f(v,\mu)$ in terms of Legendre polynomials, $P_n(\mu)$, the eigenfunctions of the collisional pitch angle scattering operator. Thus

$$f(v,\mu) = \sum_{n=o}^{\infty} A_{2n}(v,t)\, P_{2n}(\mu) \tag{11}$$

Inserting this ansatz into eq. (7) and taking the moment with respect to $P_{2k}(\mu)$, one finds the following equation for A_{2k}:

$$\frac{\partial A_{2k}}{\partial t} = \frac{1}{v^2}\frac{\partial}{\partial v}\left\{-\alpha v^2 A_{2k} + \frac{1}{2}\frac{\partial}{\partial v}(\beta v^2 A_{2k})\right\} +$$

$$+ \frac{\lambda_{2k}\gamma}{4v^2} A_{2k} + \frac{\langle P_{2k}\, Q(\Sigma A_{2n} P_{2n})\rangle}{\langle P_{2k}^2\rangle} \tag{12}$$

where λ_{2k} is the eigenvalue of the pitch angle scattering operator corresponding to P_{2k} and $\langle \quad \rangle$ denotes integration over the pitch angle variable μ.

Since $P_{2n}(\mu)$ is not an eigenfunction of the RF operator, Q, eq. (12) becomes an infinitely coupled system for the determination of $\{A_{2k}\}$. However, if the distribution $f(v,\mu)$ is almost isotropic it is meaningful to truncate the system by neglecting higher order moments, keeping only the lowest order (isotropic) moment $A_o(v,t)$. Assuming steady-state conditions we arrive at the following semi-analytical solution,

$$A_o(v) = A(0)\exp\Big(-\int_o^v \frac{-2\alpha v^2 + \frac{d}{dv}(\beta v^2)}{\beta v^2 + 2K_n v^2 F_n(v)}\,dv\Big) \tag{13}$$

where

$$F_n(v) = \frac{1}{2}\int_{-1}^{+1}(1-\mu^2)H_n\Big(\frac{k_\perp v}{\omega_{ci}}\sqrt{1-\mu^2}\Big)d\mu \tag{14}$$

Asymptotic isotropic solutions of the Fokker-Planck equation

Several informative conclusions can be drawn from asymptotic forms of eqs. (13) and (14)

(i) Fundamental ion cyclotron heating

If we neglect finite Larmor radius effects we can approximate $J_o^2(x) \simeq 1$ in which case $F_1(v) = 2/3$. Furthermore using the high and low energy asymptotic expansions of the collision coefficients we obtain, [4]

$$A_o(v) \sim \begin{cases} \exp\Big(-\dfrac{E}{T_o(1+\xi_\ell)}\Big) & E \ll E_c \\ \exp\Big(-\dfrac{E}{T_o(1+\xi)}\Big) & E \gg E_c \end{cases} \tag{15}$$

where in accordance with our previous qualitative analysis $\xi_\ell = (m_e/m_i)^{1/2}\xi$ and T_o denotes the (common) background temperature.

(ii) Second harmonic ion cyclotron heating

Approximating $J_1^2(x) \simeq x^2/4$ and keeping only second order terms in the expansion of $H_2(x)$ we obtain

$$A_o(v) \sim \begin{cases} \exp(-E/T_o) & E \ll E_c \\ \dfrac{1}{E^{1/\eta}} & E \gg E_c \end{cases} \qquad (16)$$

where

$$\eta = \frac{2}{15}\frac{K_2 k_\perp^2}{\omega_{ci}^2} t_s \equiv \frac{t_s P_M}{15n T_o} = \frac{\xi}{5} \qquad (17)$$

In eq. (17), P_M denotes the (fictitious) RF power absorbed by a Maxwellian of density n and temperature, T_o.

The asymptotic solution, eq. (16), confirms our qualitative picture of an unaffected low energy region and a strongly enhanced high energy tail. In fact, for sufficiently strong RF fields ($\eta \geq 2/3$), the tail becomes so enhanced that the distribution can no longer be normalized, indicating a run-away phenomenon. This is actually due to the parabolic approximation of $J_1^2(x)$. A better approximation of $J_1^2(x)$ for $x \lesssim 1$ is a straight line, cf. Fig. 8. In this context we emphasize that the explicit form of the high energy tail may be significantly affected also by the $|E_-|$-contribution to the RF-diffusion constant since typically $|E_-|^2/|E_+|^2 \simeq 10$, cf. [7].

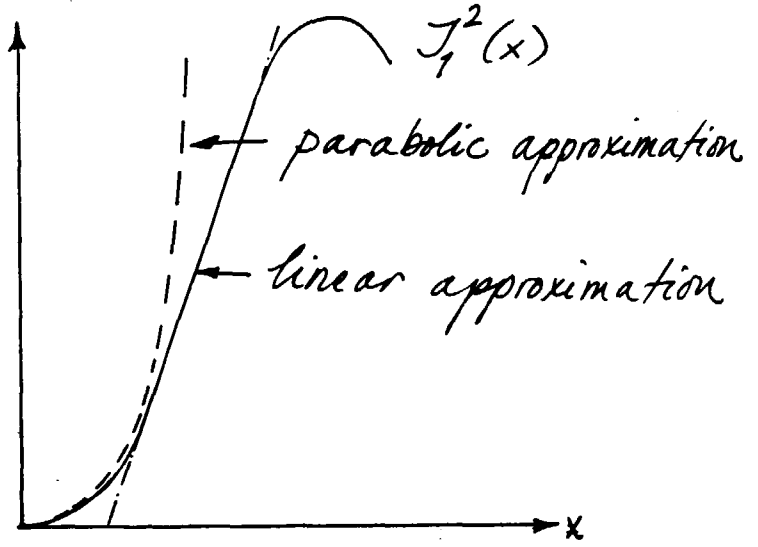

Fig. 8 Different approximations of $J_1^2(x)$.

However, if we for simplicity use the linear approximation for $J_1^2(x)$ as an approximation also for $H_2(x)$, we find the asymptotic (integrable) solution

$$A_o(v) \sim \exp\left(-\frac{v}{\eta^*}\right) \tag{18}$$

where η^* is a constant determined by the slope of the linear approximation for J_1^2. Thus, the run-away situation does not occur when the correct variation of $J_1^2(x)$ is accounted for. Nevertheless, it does indicate the formation of very strong RF-induced high energy tails and concomitant strongly enhanced RF power absorption at a certain critical field strength, cf. Fig. 9.

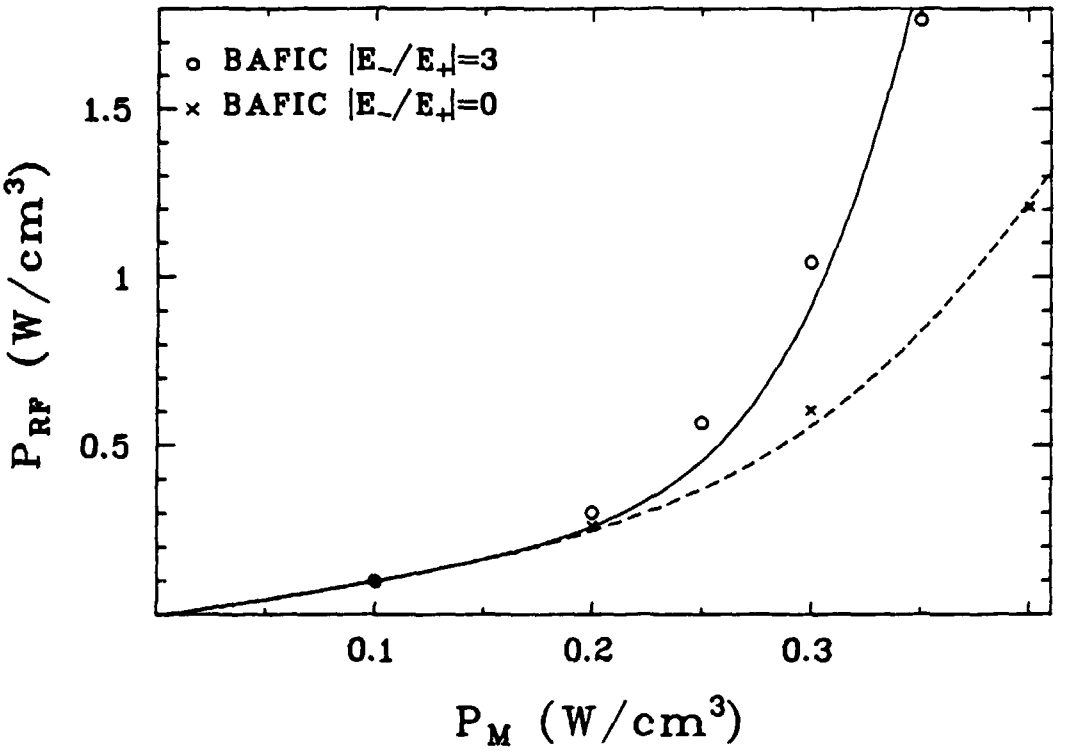

Fig. 9 Illustration of the second harmonic absorption "run away" effect, [7].

Anisotropy

The isotropic solutions discussed in the previous section are derived under the assumption that the degree of anisotropy is small so that the influence of higher order moments can be neglected. The validity of this assumption can be checked a posteriori by perturbatively determining the first anisotropic moment $A_2(v)$. This yields, [2]

(i) Fundamental heating

$$A_2(v) \sim \begin{cases} -EA_o(v) & E \ll E_c \\ -\xi A_o(v) & E \gg E_c \end{cases} \qquad (19)$$

Thus the anisotropy is small in the low energy limit and vanishes completely as $E \to 0$. However, in the high energy limit $|A_2(v)|/A_o(v) \approx \xi$, which

indicates that for strong RF power absorption ($\xi > 1$), the high energy tail becomes so strongly anisotropic so as to make inconsistent the perturbative solution procedure based on a truncated Legendre polynomial expansion.

(ii) Second harmonic heating

$$A_2(v) \sim \begin{cases} -E^2 A_o(v) & E \ll E_c \\ -\frac{10}{7} A_o(v) & E \gg E_c \end{cases} \qquad (20)$$

At low energies the distribution is very isotropic, even more so than for fundamental heating (as expected). However, the strong anisotropy in the high energy limit (independent of RF power) again invalidates the truncated expansion procedure.

Thus, we are led to the conclusion that a truncated expansion in Legendre polynomials is very useful for a description of the low energy part of the distribution, which is almost isotropic, but is not appropriate for an analysis of strongly anisotropic high energy tails.

Anisotropic high energy tail analysis

In view of the limited success of the Legendre polynomial expansion approach in describing the high energy tails it is tempting to try to make use of the simple form of the RF-diffusion operator when expressed in the variables $(v_\perp, v_\parallel)$. The form of the collision operator, expressed in these coordinates is very complicated but by restricting the analysis to the high energy, strongly anisotropic tail, important information can be obtained which complements the isotropic results.

Well out in the high energy, strongly anisotropic tail distribution the following approximations can be made

$$|v_\parallel| \ll v_\perp$$

$$v_{\parallel} \frac{\partial}{\partial v_{\parallel}} \simeq v_{\perp} \frac{\partial}{\partial v_{\perp}} \tag{21}$$

Making use of eq. (21) in the Fokker-Planck equation a new equation can be derived for the reduced distribution $F(v_{\perp})$ defined by

$$F(v_{\perp}) \equiv \int_{-\infty}^{+\infty} f(v_{\parallel}, v_{\perp}) dv_{\parallel} = \langle f \rangle \tag{22}$$

If we neglect coupling to higher order moments of the form $\langle v_i^{2n} f \rangle$ we obtain the following solution for $F(v_{\perp})$:

$$F(v_{\perp}) \sim \exp\left(- \int^{v_{\perp}} \frac{-2\alpha v_{\perp} + \frac{d}{dv_{\perp}} (\beta v_{\perp}) + \gamma/2}{\beta + 2K_n v_{\perp}^2 H_n(k_{\perp} v_{\perp}/\omega_{ci})} dv_{\perp}\right) \tag{23}$$

which is strongly reminiscent of the isotropic solution, eq. (13). The main differences are: (i) the pitch angle scattering term ($\gamma/2$) in the numerator which enhances the friction force and (ii) the RF-diffusion is stronger since the absorbed RF power is no longer assumed to be isotropized.

The asymptotic high energy distributions are found to be

$$F(v_{\perp}) \sim \begin{cases} \exp\left[- \frac{E_{\perp}}{T_o(1+3\xi/2)}\right] & (\omega = \omega_{ci}) \\ \frac{1}{E_{\perp}^{8/15\eta}} & (\omega = 2\omega_{ci}) \end{cases} \tag{24}$$

These solutions agree in form with the corresponding isotropic results, eqs. (15) and (16) except for higher "temperatures" ($\xi \to 3\xi/2$ and $\eta \to 15/8\eta$ respectively).

A decisive drawback of this analysis is the fact that it does not, in a consistent manner join the low energy isotropic distribution. Thus, eq. (23) yields the correct asymptotic form of the distribution, but its

proper height is left undecided. Nevertheless, the solution (23) gives important complementary information about the properties of the strongly anisotropic high energy tails. As an illustrative example we show in Fig. 10 a comparison between full 2D-numerical calculations and the variation of the local temperature (defined as $-(d/\ln A_o(v)/dv)^{-1}$). Note the transition from the isotropic temperatures at low energies to the anisotropic temperatures at high energies.

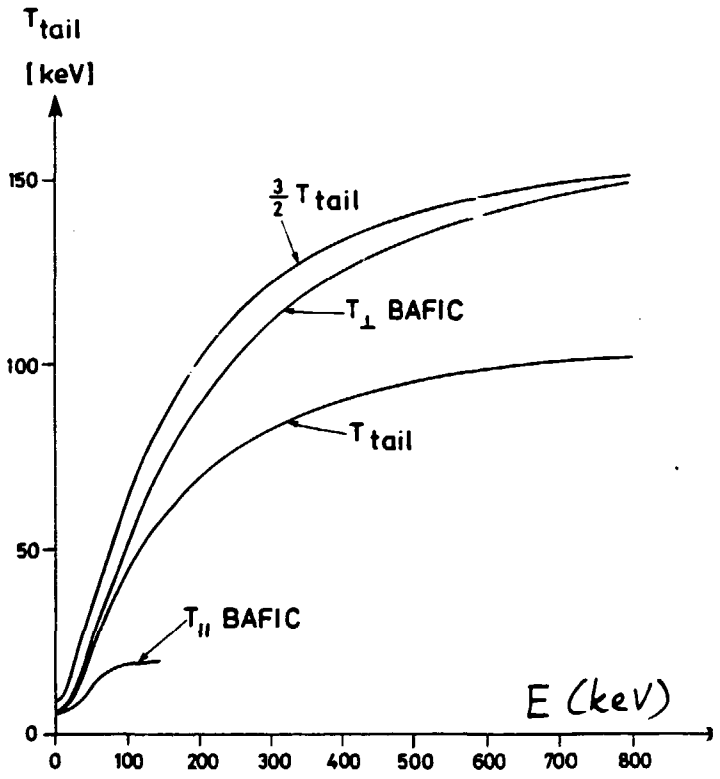

Fig. 10 Local tail temperatures, [7].

Velocity space averages

The situation so far represents a stalemate: we have the isotropic result based on a truncated expansion in Legendre polynomials, which gives a good description of the low energy bulk distribution, but which does not give a good representation of the tail. On the other hand, the anisotropic approach gives a correct picture of the high energy tail but leaves a constant of proportionality (the height) undetermined and the fundamental

assumptions of the approach excludes an extension to the low energy isotropic part of the distribution.

However, in many situations the distribution function, $f(v,\mu)$, itself is not the goal but only the means to evaluate certain velocity space averages representing physically meaningful quantities, i.e.

$$\langle\langle G(v,\mu)\rangle\rangle \equiv \int G(v,\mu) f(v,\mu) d^3v \tag{25}$$

Example of such averages are:

(i) absorbed RF power

$$G = \frac{1}{2} mv^2 \tag{26}$$

(ii) RF power collisionally transferred to electrons and background ions

$$G = \frac{1}{2} mv^2 C_e(v) \; ; \qquad G = \frac{1}{2} mv^2 \, C_i(v) \tag{27}$$

where C_e and C_i denotes the contributions to the collisional friction operator coming from electrons and background ions respectively.

(iii) fusion reactivity

$$G = \sigma(v)v \tag{28}$$

In particular we note that if G is independent of μ, cf eqs. (26)-(28), eq. (25) can be rewritten as

$$\langle\langle G\rangle\rangle = \int G(v) 4\pi v^2 dv \, \frac{1}{2} \int_{-1}^{+1} f(v,\mu) d\mu =$$

$$= \int G(v) \langle f\rangle \, 4\pi v^2 dv \tag{29}$$

where <f> denotes the pitch angle averaged distribution.

Obviously, if f is represented in terms of a Legendre polynomial expansion, then $\langle f \rangle = A_o(v)$ - the isotropic part of f. This implies that even if the isotropic part of f ($A_o(v)$) may not be a very good approximation of the actual distribution ($f(v,\mu)$) for all energies, it should still be a very good approximation for the evaluation of velocity space averages, except possibly in situations where the weighting function is strongly μ-dependent and/or strongly peaked at high energies.

As a matter of fact, this conjecture is verified in a manner which exceeds expectations in [5-8]. It turns out that the isotropic solution $A_o(v)$, as given by eqs. (13) and (14) provides useful and accurate results for most physically meaningful velocity space averages including such high energy characteristics as fusion reactivity and absorbed power. Examples of the agreement with full 2D numerical computations are given in Figs. 11-13

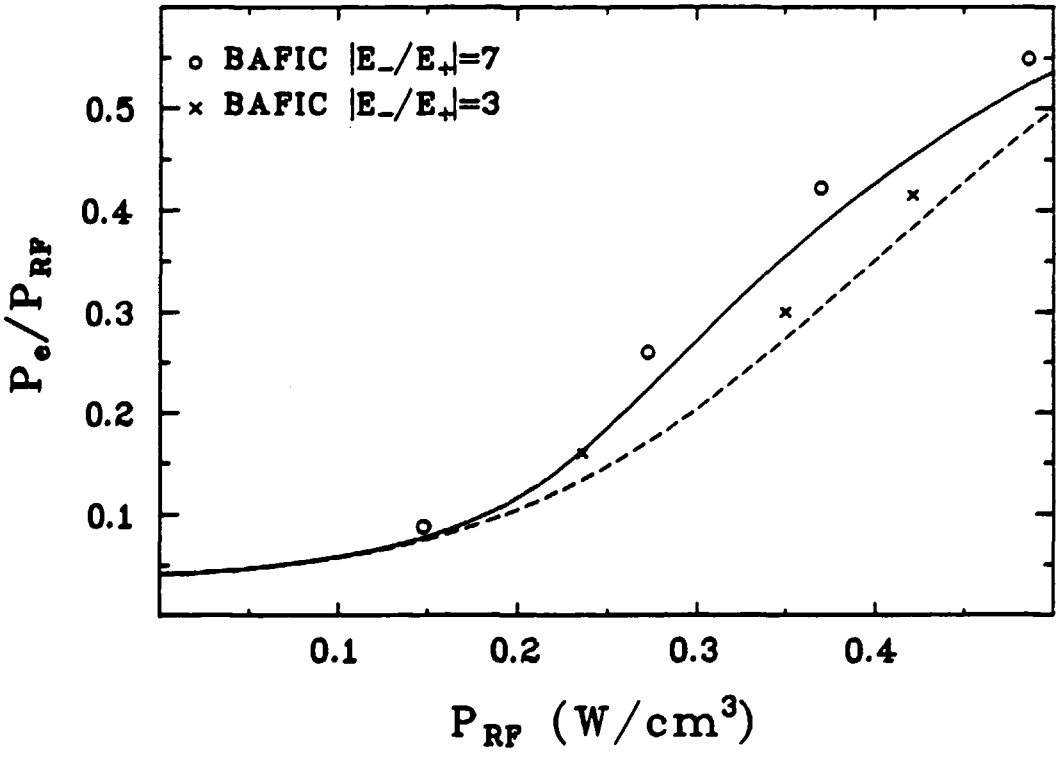

Fig. 11 Comparison between full 2D numerical results and the results from the isotropic analysis, [5] for the collisional power transfer to the electrons.

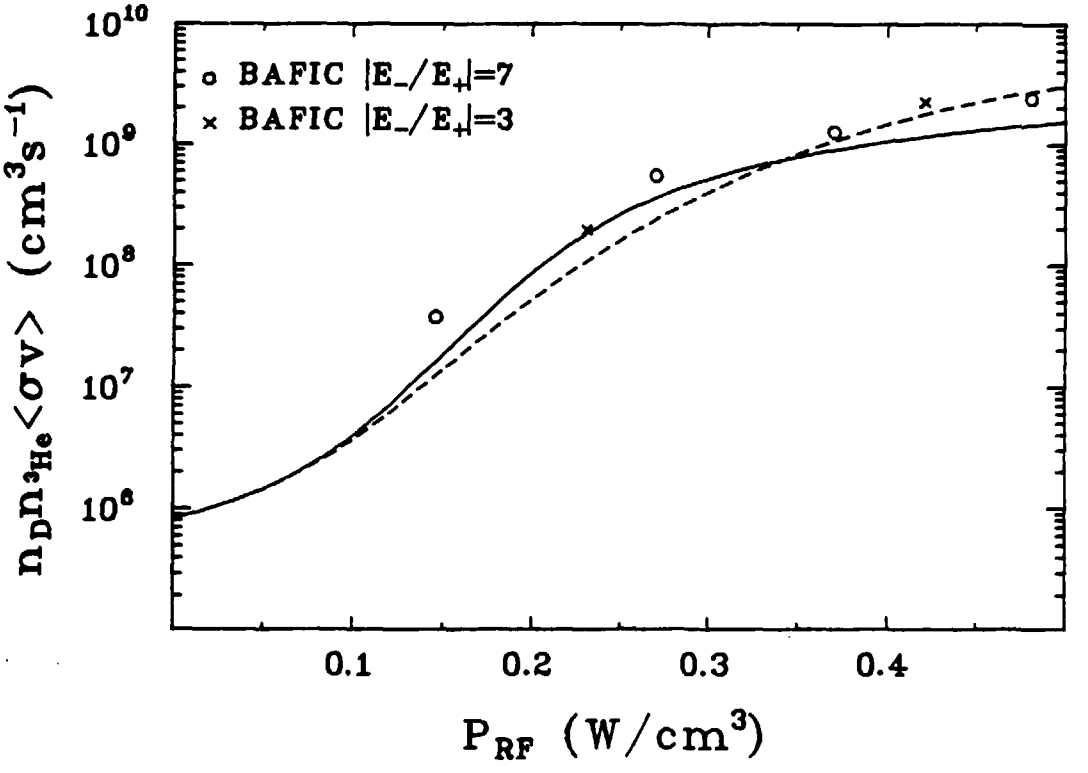

Fig. 12 Comparison of fusion rates for the D+ ^{3}He reaction (minority heating), [5].

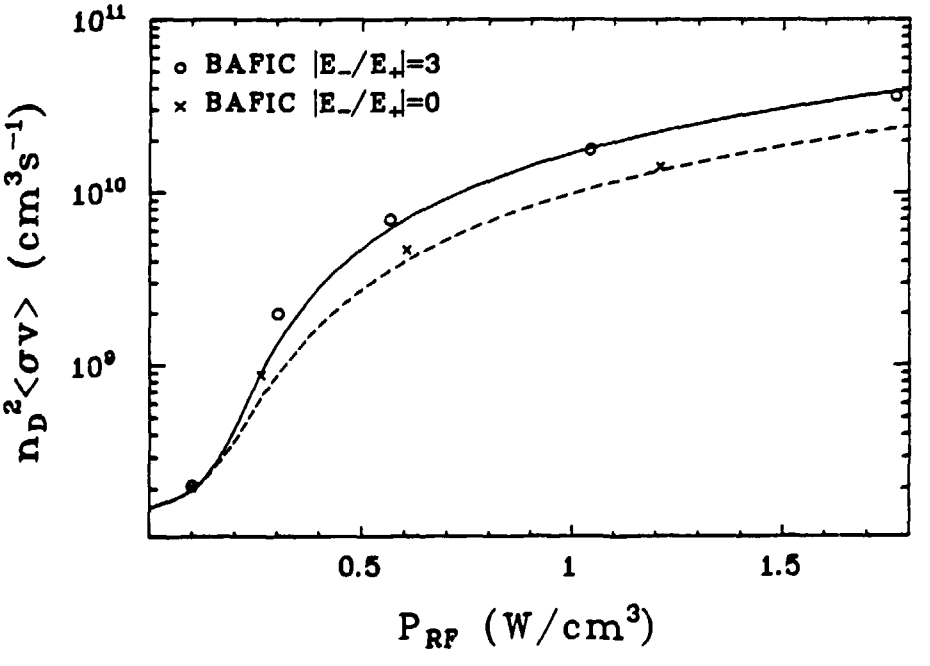

Fig. 13 Comparison of fusion rates for the D+D reaction (second harmonic heating), [5].

Surprisingly good agreement is obtained even for such tail sensitive quantities as the number of tail particles, n_t, and the tail contribution to the total β-value, β_t, cf Figs. 14-15. The tail is defined by subtracting from f a Maxwellian with the same temperature as the low energy part.

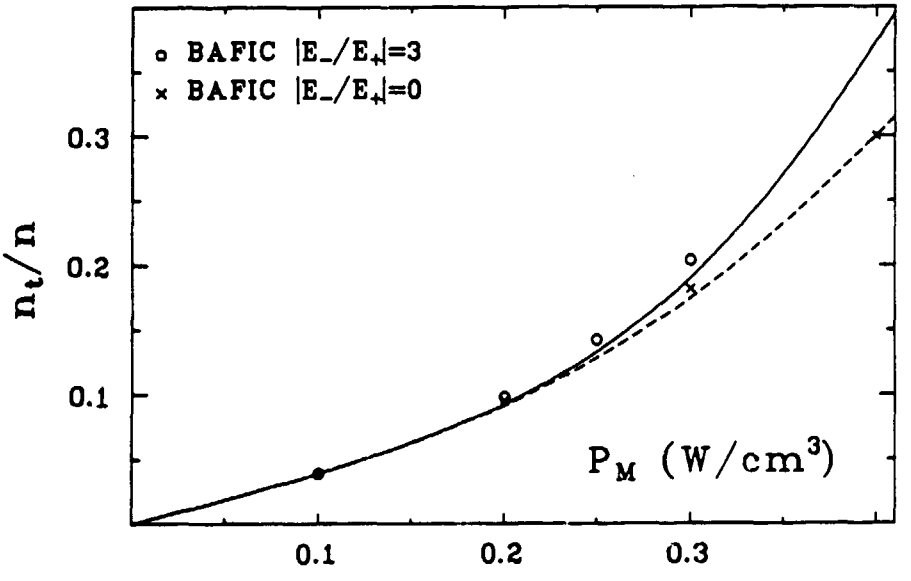

Fig. 14 Comparison of number of tail particles obtained by the isotrop analysis and full 2D calculations, [5].

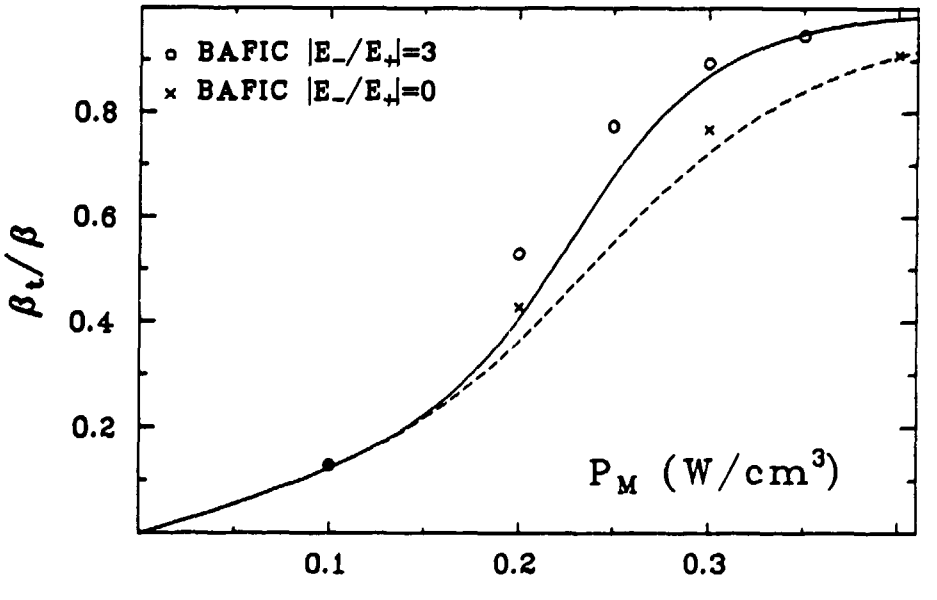

Fig. 15 Comparison of the tail contribution to the β-value, as obtained by the isotropic analysis and full 2D calculations, [5].

The isotropic analysis has also been extended [6-8] to include the case of combined NBI and ICRF heating with the RF wave frequency tuned to the cyclotron frequency of the injected ions, a relevant heating scenario for JET. The corresponding Fokker-Planck equation, eq. (7), is then augmented with a source term $S(v,\mu)$ and a loss term $L(v,\mu)$ accounting for the injection and the loss of particles. An example of the corresponding isotropic approximation of the distribution in this case is given in Fig. 16.

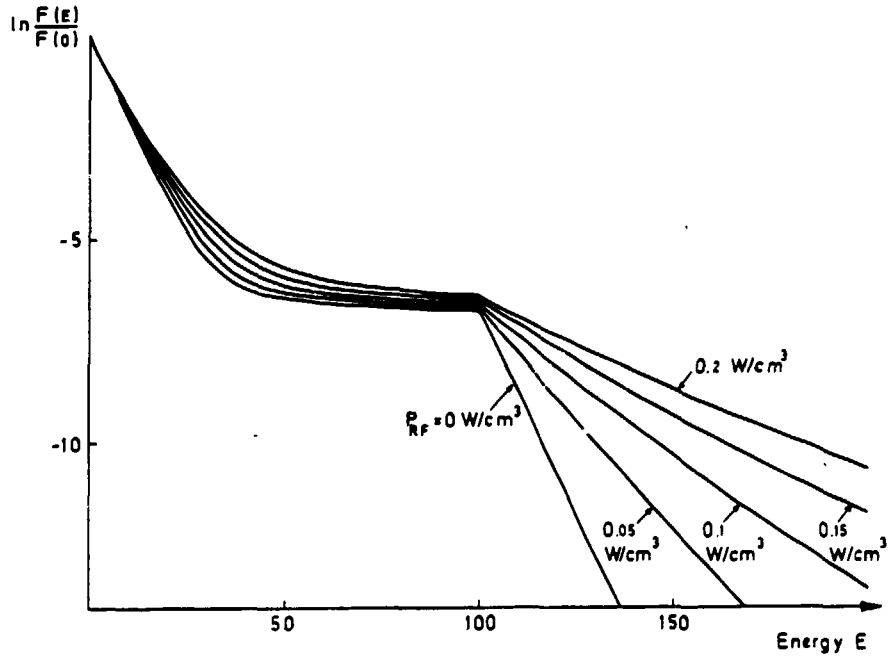

Fig. 16 Example of an isotropic approximation of the distribution of RF heated beam injected ions, [9].

Again the isotropic approximation is a useful means for evaluating velocity space averages, even in cases involving strongly anisotropic injection sources, cf Figs. 17-19.

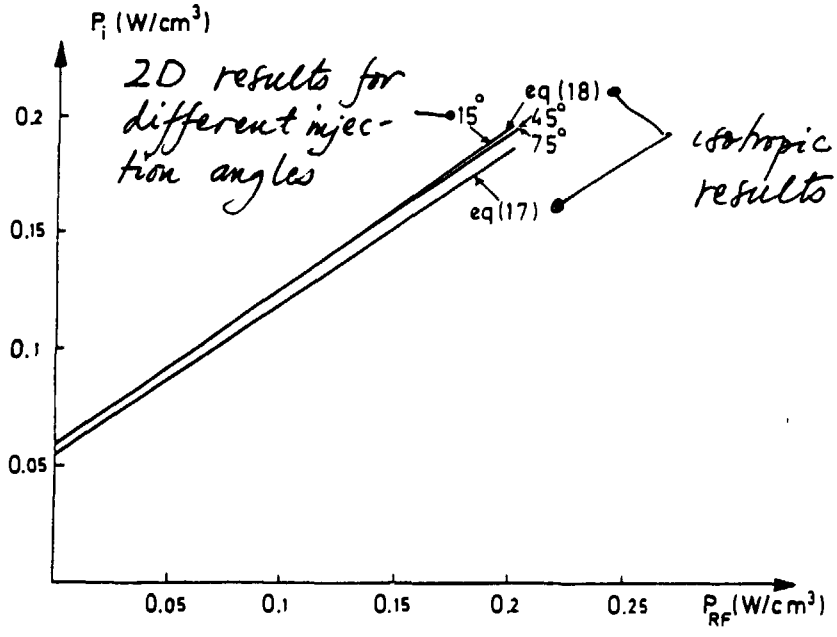

Fig. 17 Collisional power transfer to background ions for an energy clamping situation, [9].

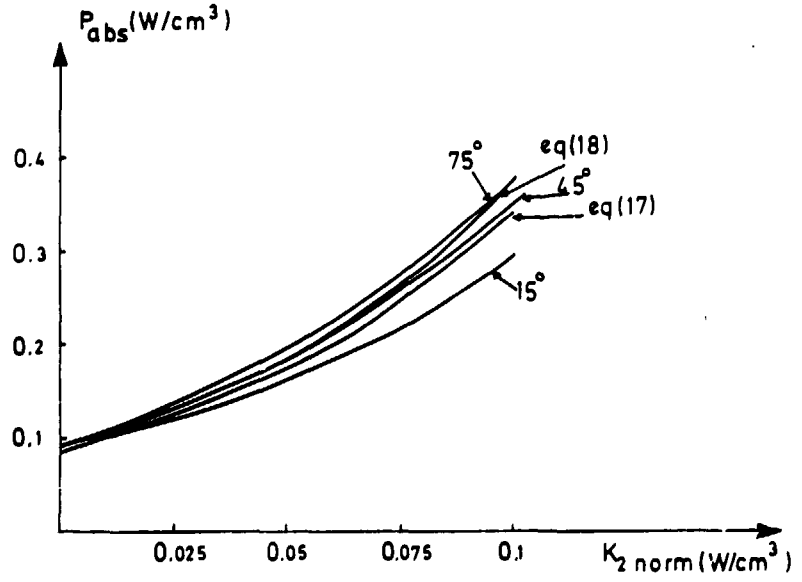

Fig. 18 Absorbed RF-power for an energy clamping situation, [9].

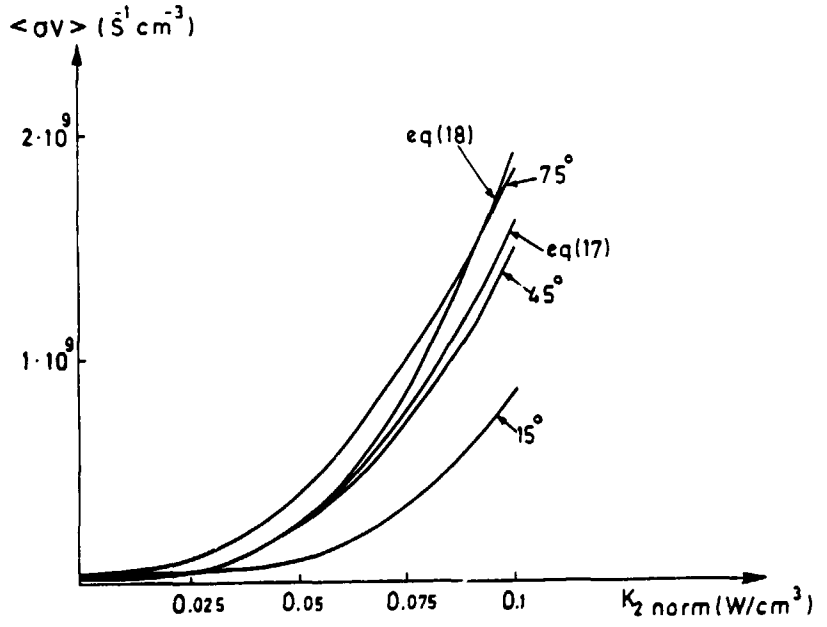

Fig. 19 Fusion reactivity (^{3}He injected into D), [9].

Influence of higher order finite Larmor radius effects

Previous approximations of the RF-induced diffusion constant have employed first order expansions of $J^2_{n-1}(x)$. However, for certain heating scenarii on JET, deviations from, e.g. the parabolic approximation of $J^2_1(x)$ starts to develop already for energies E ≈ 50 kev. It is therefore important to incorporate higher order finite Larmor radius effects, in particular for the correct interpretation of absorbed RF power and fusion measurements. The importance of FLR-effects in saturating the run-away phenomenon for second harmonic heating has already been emphasized.

In an expansion to higher order in $k_\perp$ it is important to keep the contributions to the diffusion constant coming from the right hand component, E_-, of the wave since typically $|E_-|/|E_+| \gg 1$. As an illustration of this effect we note that to fourth order in $k_\perp$ we obtain for fundamental heating, cf. [7]

$$H_1(u_\perp) = |E_+|^2(1-u_\perp^2+(5+\Lambda)u_\perp^4/64)$$

where $u_\perp = k_\perp v_\perp/\omega_{ci}$ and $\Lambda \equiv |E_-|^2/|E_+|^2$. This result implies that the reduction of the diffusion constant which is due to the $J_o^2(x)$ variation is replaced by an enhancement due to the increasing $J_2^2(x)$ contribution if $(5+\Lambda)/64 \gg 1/2$, i.e. if $|E_-|/|E_+| > 5$, cf. fig. 22.

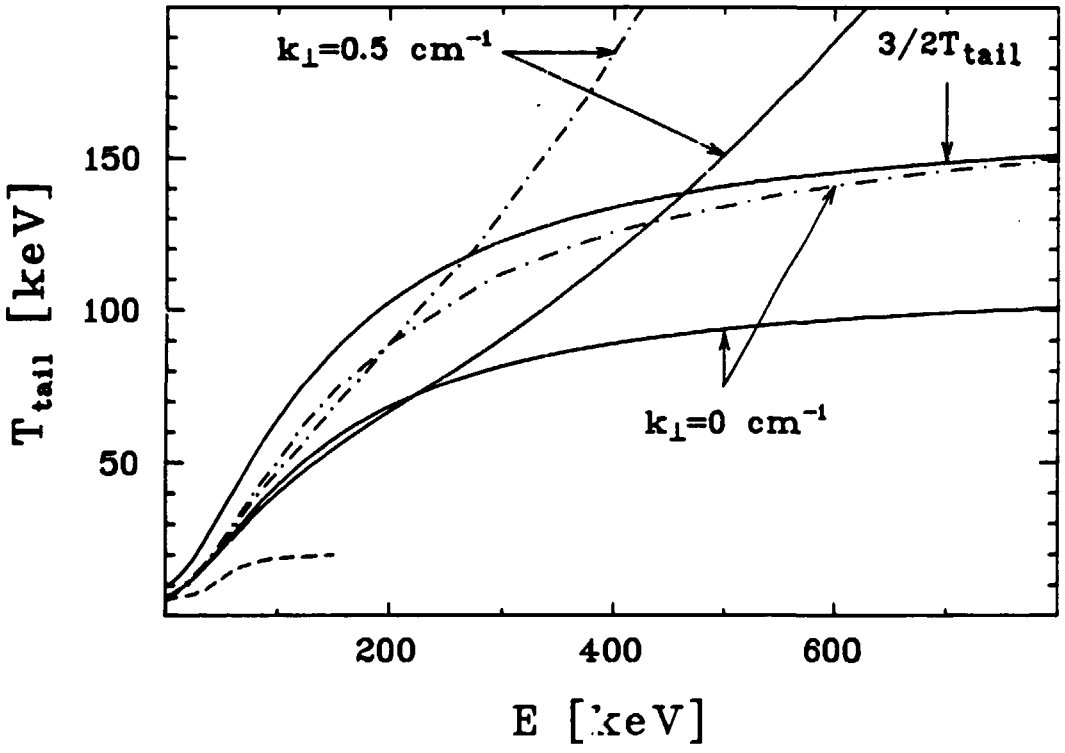

Fig. 20 Illustration of the effect of finite $k_\perp$ on the local temperature, [5], for fundamental heating.

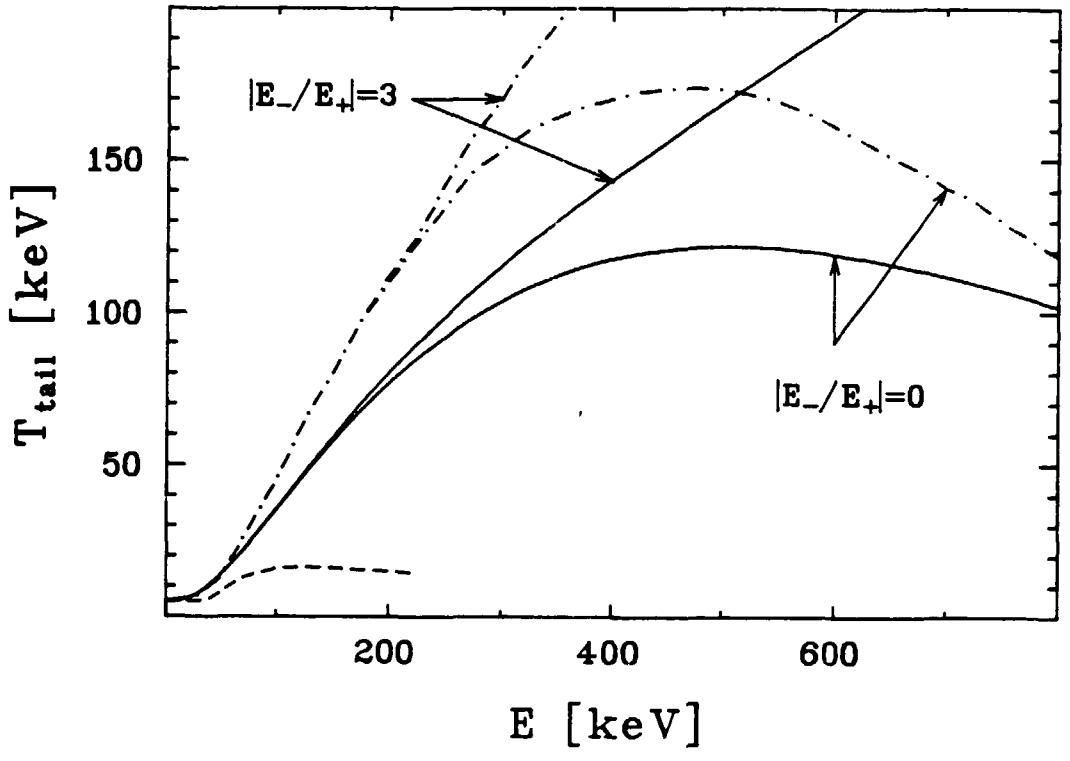

Fig. 21 Illustration of the effect of finite $|E_-|/|E_+|$ on the local temperature for second harmonic heating, [7].

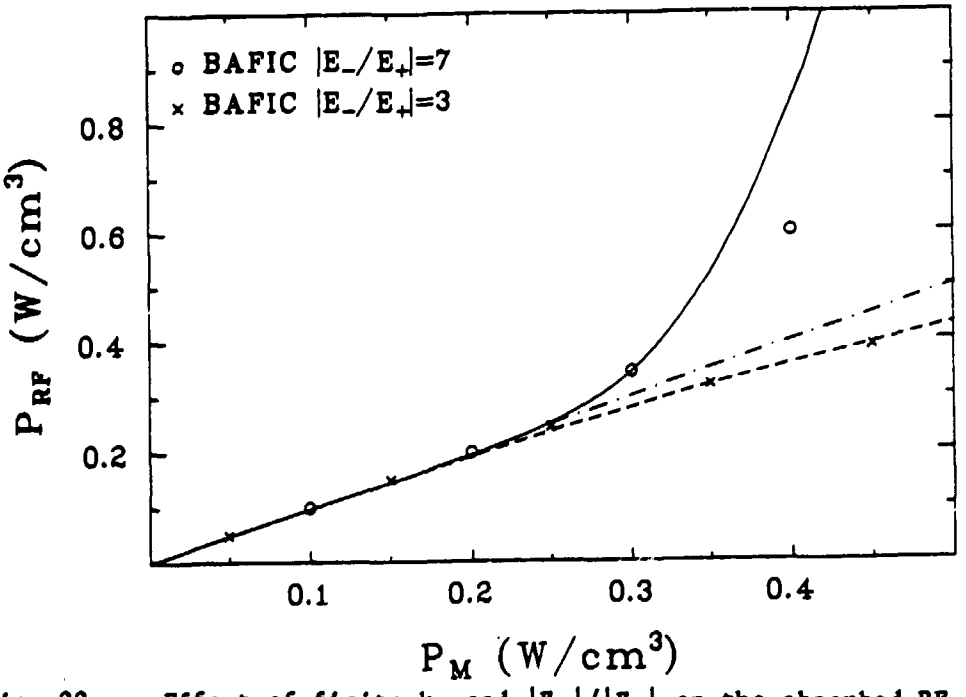

Fig. 22 Effect of finite $k_\perp$ and $|E_-|/|E_+|$ on the absorbed RF power, [7].

Direct approach to pitch angle averaged distributions

In our previous analysis we have tried to determine the full distribution function $f(v,\mu)$, but then in practice we only used the pitch angle averaged (isotropic) part in the determination of the velocity space averages. An alternative approach would be to derive an equation for $\langle f \rangle$ itself, hoping to find a significant simplification.

We restrict the present analysis to fundamental heating and neglect FLR effects. By pitch angle averaging the Fokker-Planck equation we find an equation of the following form. cf [10,11]:

$$L_1(v, \frac{d}{dv})\langle f \rangle = L_2(v, \frac{d}{dv})\langle \mu^2 f \rangle \tag{30}$$

where L_1 and L_2 are certain inhomogeneous differential operators. Eq. (30) again implies a coupling to higher order moments, which we, however, can formally truncate by writing

$$\langle \mu^2 f \rangle \equiv \mu^2_{eff}(v)\langle f \rangle \tag{31}$$

This yields a self-consistent equation for $\langle f \rangle$ of the form:

$$L(v, \frac{d}{dv})\langle f \rangle = 0 \tag{32}$$

which can be solved to give

$$\langle f \rangle \sim \exp\{- \int_0^v \frac{-\alpha v^2 + \frac{1}{2}\frac{d}{dv}(\beta v^2) + K_1 v[1-3\mu^2_{eff} - v\frac{d}{dv}(\mu^2_{eff})]}{[\frac{1}{2}\beta + K_1(1-\mu^2_{eff})]v^2} dv\} \tag{33}$$

Provided $\mu^2_{eff}(v)$ is known, eq. (33) constitutes an explicit (and exact) solution for $\langle f \rangle$. The qualitative variation of $\mu^2_{eff}(v)$ is easily inferred since

$$\mu^2_{eff} = \frac{\langle \mu^2 f \rangle}{\langle f \rangle} \rightarrow \begin{cases} 1/3 & \text{for isotropic distributions} \\ 0 & \text{for strongly anisotropic distributions} \end{cases}$$

Thus, for the RF-distorted distribution we expect $\mu^2_{eff} \to 1/3$ as $v \to 0$ and $\mu^2_{eff} \to 0$ as $v \to \infty$. Indeed, if we take these limits in eq. (33) we regain our previous isotropic and anisotropic solutions respectively. Since the distribution remains essentially isotropic up to characteristic energies $E \simeq E_\gamma = \frac{1}{2} m v_\gamma^2$, where v_γ is the characteristic pitch angle scattering velocity, [1,2] we have used the following simple function model for μ^2_{eff}:

$$\mu^2_{eff}(v) = \frac{1}{3} \exp\left(-\left(\frac{v}{v_*}\right)^4\right) ; \quad v_* = 0.55\, v_\gamma \tag{35}$$

The corresponding result for $\langle f \rangle$ relates, in a consistent manner, the previously unrelated isotropic and anisotropic approaches.

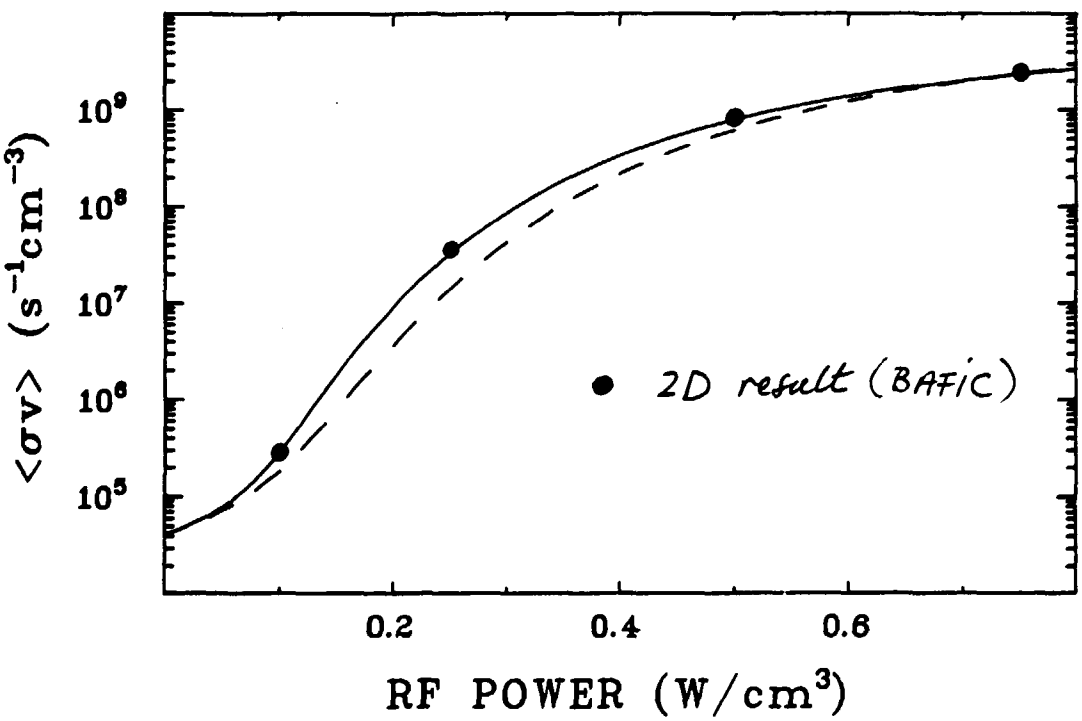

Fig. 23 Comparison between fusion rates (He^3+D) obtained by the anisotropic, the isotropic and full 2D numerical computations, [11].

Effects of particle trapping on ICRH

The original analysis of Stix, [1], involved an averaging over magnetic surfaces. This averaging did not, however, take into account the modulation of $v_{\parallel}$ and $\mu = v_{\parallel}/v$ that the particle experiences due to toroidal effects, even less the possibility of trapped particles. In [12] we derived a new bounce averaged Fokker-Planck equation which included these effects on, in particular, the RF diffusion operator. Although the resulting equation is quite complicated certain qualitative features are easily discernible:

(i) Particles that have the turning points of their banana orbit outside the resonance layer will not absorb RF power

(ii) the RF-induced diffusion transfers particles towards higher $v_{\perp}$, i.e. increases the number of trapped particles

(iii) the combined effect of (i) and (ii) is to cause a pile up in velocity space around the pitch angle corresponding to the situation when the tips of the particles banana orbit touch the resonance layer, cf. Fig. 24

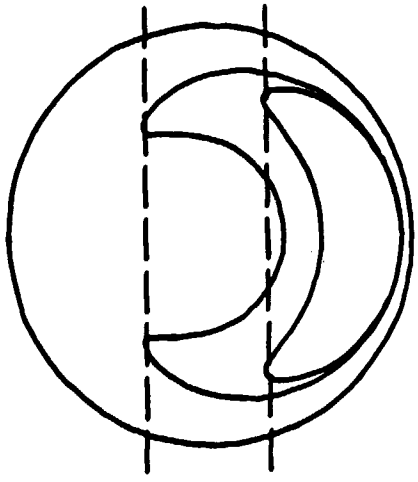

Fig. 24 Illustration of the ICRH-enhanced trapping.

This pile up effect should show up as a horn like deformation of the level curves of f, as shown qualitatively in Fig. 25.

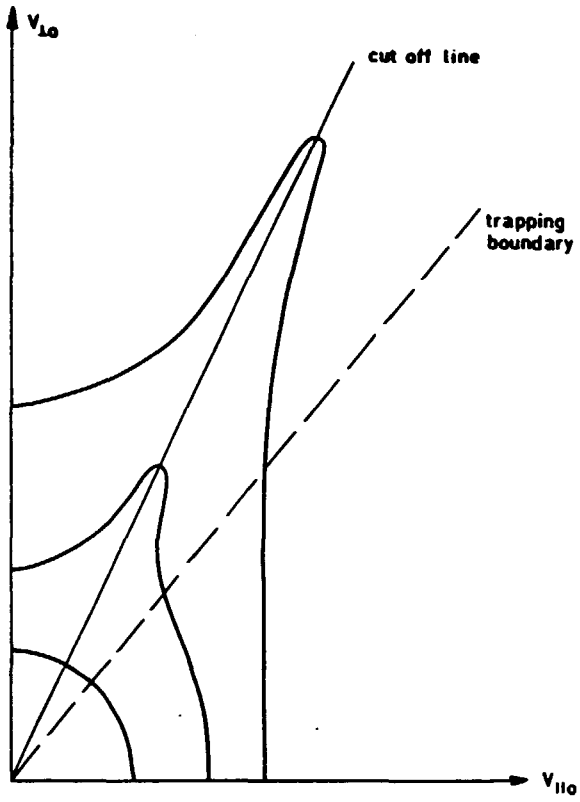

Fig. 25 Qualitative plot of the level curves in the presence of trapping effects, [14].

Corresponding inversions of the distribution function with pitch angle have also been observed experimentally, Fig. 26.

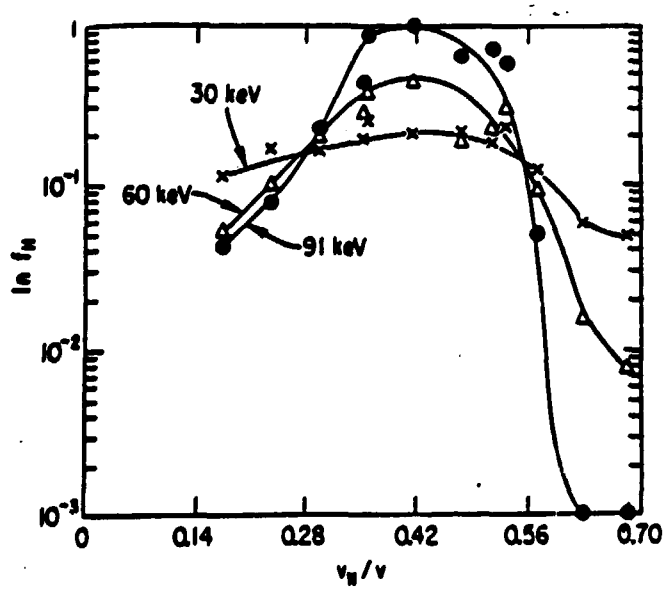

Fig. 26 Experimentally measured pitch angle dependence, [19].

In [13] we have rigorously analyzed the bounce averaged Fokker-Planck equation for minority heating using a perturbative expansion in terms of the eigenfunctions of the pitch angle scattering operator. The analysis is complicated involving Legendre polynomials with non-integer indices and the matching of solutions at the RF cut-off boundary in velocity space. The main results are that toroidal effects tend to reduce the overall anisotropy of the distribution but have little influence on the isotropic low energy part of f. This also implies that toroidal effects cannot be expected to significantly affect velocity space averages of the form discussed previously. A confirmative example of this conclusion is given in Fig. 27

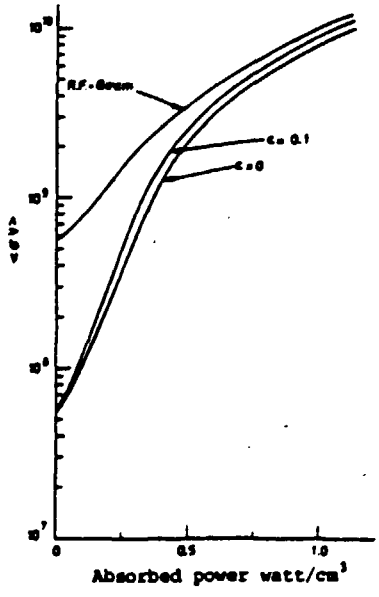

Fig. 27 Effect of particle trapping on fusion reactivity, [17].

Collisionless short time evolution of RF-heated distributions

Problems connected with RF-enhanced sawtooth activity involves inherently short timescales and have focussed the interest on the short time development of RF-heated ion distributions. However, the corresponding knowledge is much more incomplete and in [14,15] we have derived explicit analytical solutions for the short time (collisionless) development of ion distributions for several different heating scenarii. The analysis neglects collisions and is consequently only valid for times less than a slowing down, t_s. This should not be a serious limitation in connection with, e.g. sawtooth phenomena which occur on a timescale, t_{st} of typically 20 ms with the high energy particles often being expelled from the heated plasma at the sawtooth collapse, thus "resetting" the heated distribution. Since the tail formation time, t_o, is typically of the order of a few ms (for $n_e=1.5\cdot10^{12}$ cm^{-3}, T=3 kev, and $R_{RF}=0.25$ W/cm^3 we obtain $t_o\simeq3$ ms, cf eq. (4)) while the slowing down time is $t_s\sim200$-300 ms, we have the ordering $t_o\ll t_{st}\ll t_s$, which establishes the applicability of the results obtained in [14,15].

The equation we consider is

$$\frac{\partial f}{\partial t} = \frac{1}{v_\perp}\frac{\partial}{\partial v_\perp}\left(\tilde{K}_n v_\perp^{2n-1}\frac{\partial f}{\partial v_\perp}\right) + S \qquad (36)$$

where $\tilde{K}_1=K_1$, $\tilde{K}_2=K_2k_\perp^2/(4\omega_{c1}^2)$, and S represents the source function in the case of combined NBI and ICRH.

The solution of eq. (36) in the case of minority heating served as a basis for our qualitative discussion of the effect of ICRH on the distribution of the heated ions, cf eq. (3).

For second harmonic majority heating the formal solution of eq. (36), for an initially Maxwellian distribution, is not very explicit. It is more illuminating to consider the evolution of a waterbag approximation of the initial distribution. The corresponding solution for the perpendicular distribution, $F(v_\perp,t)$, is

$$F(v_\perp,t) \sim \mathrm{erfc}\left(\frac{\ln(\frac{v_\perp}{\sqrt{2}v_t})^2 + \tau}{2\sqrt{\tau}}\right) \qquad (37)$$

where $\tau = 4\tilde{K}_2 t \equiv \frac{2t}{t_2}$ and erfc denotes the complementary error function, Fig. 28 illustrates the evolution of the distribution. Note in particular the unchanged low energy region and the strong tail enhancement.

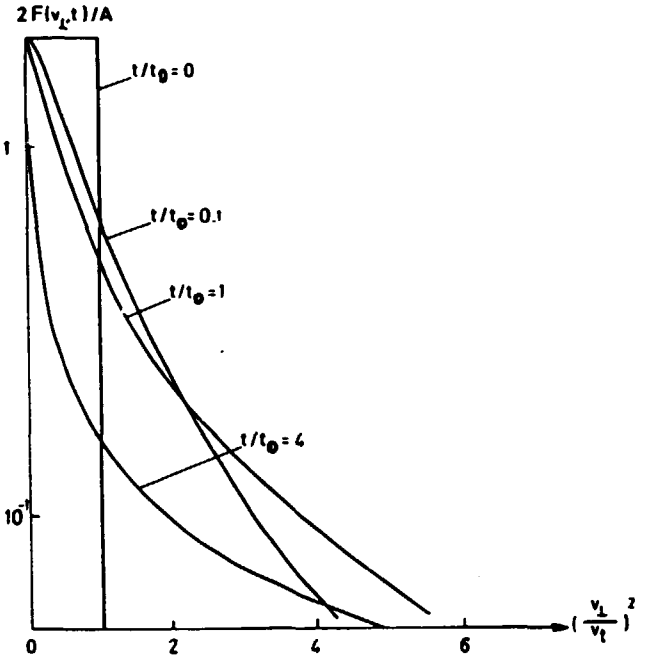

Fig. 28 Time evolution of a water bag distribution in the case of second harmonic heating, [14].

Whereas for minority heating the RF power absorption is constant (depending only on the number of particles) for second harmonic majority heating, the absorbed RF power increases exponentially with time according to

$$P_{RF} = \frac{nT}{t_2} \exp\,(t/t_2) \qquad (38)$$

Similar explicit and/or semi-explicit analytical solutions can be given for energy clamping situations involving beam sources assumed monochromatic in perpendicular energy. An example of the time evolution of an RF-heated beam distribution is given in Fig. 29. Note in particular that in addition to the RF-induced tail formation, an enhanced diffusion towards lower energies also occurs, which should manifest itself as an anomalous slowing down effect in situations where the tail formation time is significantly smaller than the slowing down time.

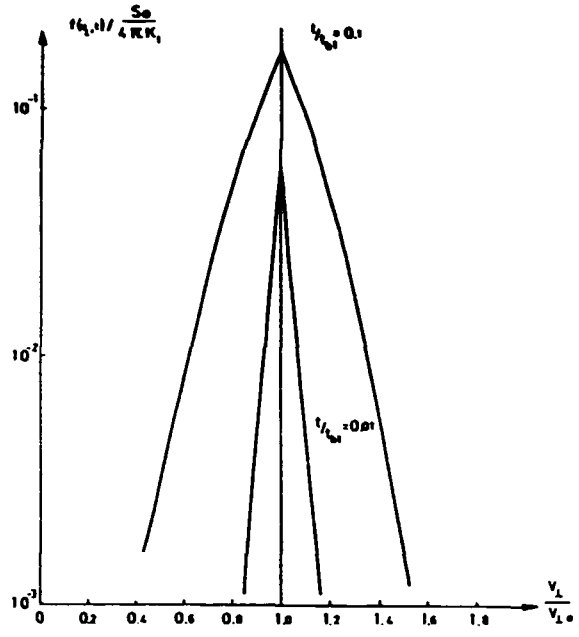

Fig. 29 Time evolution of an RF-heated beam injected distribution, [14].

A curious artifact of the time dependent solution in the case of second harmonic heating of a beam is that the height of the beam distribution at the injection energy does not, as in the case of fundamental heating, increase unboundedly in time but rather saturates at a finite value. This again illustrates the strong tail forming property of second harmonic heating.

An analysis of the time evolution of the distribution function including toroidal effects shreds further light on the form and properties of the pile up at the RF cut-off line in velocity space. It can be shown, [14], that the level curves in the case of minority heating evolve according to

$$\frac{v_{\parallel 0}^2}{v_t^2} + \frac{v_{To}^2}{v_t^2}\left(\frac{B_R/B_o}{1+t/t_o} - 2\varepsilon \sin^2\frac{\Theta_R}{2}\right) \approx \ln\frac{\text{constant}}{(1+t/t_o)} \qquad (39)$$

where index 0 denotes that the velocity coordinates are taken in the equatorial plane of the plasma cross section, index R denotes values evaluated at the resonance layer, and ε is the inverse aspect ratio.

The initially circular level curves are deformed into successively more elongated ellipses, which at a finite time, t_h, transform into hyperbolas. The characteristic time t_h is determined by

$$t_h = \frac{t_o}{2\varepsilon \sin^2 \theta_R/2} \tag{40}$$

The asymptotes of the hyperboles lie in the cut-off region in velocity space but approaches the cut-off line as time increases. This implies a run-away phenomenon in time.

However, collisional effects will again stop this development and the importance of the run-away phenomena is determined by the ratio

$$\frac{t_s}{t_h} = \frac{t_s}{t_o} 2\varepsilon \sin^2 \theta_R/2 \tag{41}$$

Thus, in the bulk region where the slowing down time is small and $t_s/t_h \ll 1$ we expect the ordinary almost circular stationary level curves. However, the elongation can be expected to increase with energy and for realistic RF-power absorption and aspects ratios (e.g. $t_s/t_o=20$, $\theta_R=\pi/2$, and $\varepsilon=0.1$) the high energy level curves should correspond to the hyperbolic situation. In addition, collisional pitch angle scattering should "round off" the subsequent strong gradients and lead to a hornlike form of the level curves around the cut-off line, as qualitatively shown in Fig. 25.

The good agreement of this qualitative picture with the result of full 2D numerical calculations is illustrated in Fig. 30.

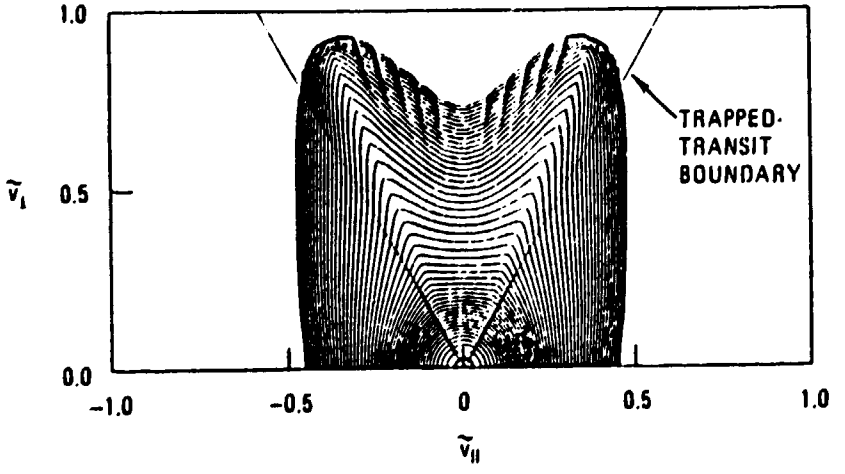

Fig. 30 Numerically obtained level curves in the presence of trapping effects, [20].

Conclusion

The main results of the work performed within the contract are:

(i) Simple analytical and/or semi-analytical expressions have been derived for the isotropic part of ion distributions heated by ICRH and also for energy clamping schemes involving both NBI and ICRH.

(ii) These isotropic expressions have been shown to be a useful and accurate means to evaluate most physically meaningful velocity space averages. They furthermore only require short computational procedure and are ideally suited for use in situations where the distribution function itself is not the final goal but the means to evaluate other physical characteristics, e.g. in transport codes.

(iii) Finite Larmor radius corrections to the RF-induced diffusion constants have been shown to significantly affect the formation of high energy tails and to play an important role for the interpretation of, eg. absorbed RF power and fusion yield data.

(iv) A new bounce averaged Fokker-Planck equation has been derived which takes into account toroidal effects on the particle velocity. This equation has subsequently been solved perturbatively in the limit of an almost isotropic distribution. This result, together with the result of a collisionless analysis, indicate that although toroidal effects could lead to important changes in the high energy characteristics of the distribution, the isotropic part is not significantly affected and consequently neither is the physically important velocity space averages.

(v) Explicit solutions have been derived which describe the collisionless short time development of ion distributions subject to RF-induced velocity space diffusion. The results should be particularly useful for sawtooth applications.

Finally, we want to emphasize that an important result of the present work is undocumented but may well turn out to be the most valuable: the increased understanding and the physical intuition, which the involved people, both at CTH and JET, have acquired of the influence of ICRH on the distribution functions of the heated ions and the subsequent interaction with the background plasma. In this context we also gratefully acknowledge the inspiring role played for the present work by T. Hellsten, W. Core and H. Hamnén at JET, who by direct collaboration and/or numerous informative discussions have contributed to the present understanding.

References

[1] T.H. Stix, Nucl. Fus. 15 (1975), 737.

[2] D. Anderson, L.-G. Eriksson, and M. Lisak, CTH-IEFT/PP-1984-18.

[3] D. Anderson, L.-G. Eriksson, M. Lisak, L.-O. Pekkari, and E. Tennfors, in Plasma Physics and Controlled Nuclear Fusion Research 1984 (Proc. 10th Int. Conf. London, 1984), Vl. 1, IAEA, Vienna (1985), 591.

[4] D. Anderson, L.-G. Eriksson, and M. Lisak, Nucl. Fus. 25 (1985), 1751.

[5] D. Anderson, W. Core, L.-G. Eriksson, H. Hamnén, T. Hellsten, and M. Lisak, CTH-IEFT/PP-1986-02

[6] D. Anderson, W. Core, L.-G. Eriksson, H. Hamnén, M. Lisak, 13th European Conf. on Contr. Fusion and Plasma Heating, Schliersee, FRG, 14-18 April, 1986, paper Mo-16, p. 103.

[7] D. Anderson, W. Core, L.-G. Eriksson, H. Hamnén, T. Hellsten, M. Lisak (submitted to Nuclear Fusion).

[8] D. Anderson, L.-G. Eriksson, and M. Lisak, W. Core, H. Hamnén, and T. Hellsten, Fusion Theory Meeting, Wepion, Belgium, June 16-18 1986) Paper 36.

[9] D. Anderson, L.-G. Eriksson, M. Lisak, W. Core, H. Hamnén, and T. Hellsten, CTH-IEFT/PP-1986-04.

[10] D. Anderson, L.-G. Eriksson, and M. Lisak, CTH-IEFT/PP-1986-08.

[11] D. Anderson, L.G. Eriksson, and M. Lisak, CTH-IEFT/PP-1986-09.

[12] D. Anderson, M. Lisak, and L.-O. Pekkari, Phys. Fluids 28 (1985), 3590.

[13] D. Anderson and M. Lisak, J. Plasma Phys. 35 (1986), 107.

[14] D. Anderson, L.-G. Eriksson, and M. Lisak, CTH-IEFT/PP-1986-01 (also to be published in J. Plasma Phys.).

[15] D. Anderson, L.-G. Eriksson, and M. Lisak, Fusion Theory Meeting, Wépion, Belgium, June 16-18 (1986), paper 35.

[16] P.L. Colestock, S.L. Davies, J.C. Hosea, D.Q. Hwang and H.R. Thompson, Proc. 2nd Joint Grenoble-Varenna Int. Symp. (1980) Vol. 1, 471.

[17] T. Hellsten, K. Appert, W. Core, H. Hamnén, S. Succi, 12th European Conf. on Contr. Fus. and Plasma Physics, Budapest, 2-6 Sept. 1985, paper FP Tu038.

[18] D.Q. Hwang, et al, Phys. Rev. Lett. 51 (1983), 1865.

[19] R. Kaita et al, Nucl. Fus. 23 (1983), 1089.

[20] R.W. Harvey, M.G. McCoy, G.D. Kerbel, S.C. Chiu, Nucl. Fus. 26 (1986), 43.